Experimental study on the behavior of segmented buried concrete pipelines subject to ground movements

Junhee Kim[a], Jerome P. Lynch[*a], Radoslaw Michalowski[a], Russell A. Green[b], Mohammed Pour-Ghaz[c], W. Jason Weiss[c], Aaron Bradshaw[d]

[a]Dept. of Civil and Environmental Engineering, University of Michigan, Ann Arbor, Michigan;
[b] Charles E. Via, Jr. Dept. of Civil and Env. Engineering, Virginia Tech, Blacksburg, Virginia
[c] School of Civil Engineering, Purdue University, West Lafayette, Indiana;
[d] Department of Civil Engineering, Merrimack College, MA

ABSTRACT

Seismic damage to buried pipelines is mainly caused by permanent ground displacements, typically concentrated in the vicinity of the fault line in the soil. In particular, a pipeline crossing the fault plane is subjected to significant bending, shear, and axial forces. While researchers have explored the behavior of segmented metallic pipelines under permanent ground displacement, comparatively less experimental work has been conducted on the performance of segmented concrete pipelines. In this study, a large-scale test is conducted on a segmented concrete pipeline using the unique capabilities of the NEES Lifeline Experimental and Testing Facilities at Cornell University. A total of 13 partial-scale concrete pressure pipes (19 cm diameter and 86 cm long) are assembled into a continuous pipeline and buried in a loose granular soil. Permanent ground displacement that places the segmented concrete pipeline in compression is simulated through the translation of half of the soil test basin. A dense array of sensors including linear variable differential transducers, strain gauges, and load cells are installed along the length of the pipeline to measure its response to ground displacement. Response data collected from the pipe suggests that significant damage localization occurs at the ends of the segment crossing the fault plane, resulting in rapid catastrophic failure of the pipeline.

Keywords: pipeline, concrete pipe, permanent ground displacement, wireless sensor, instrumentation

1. INTRODUCTION

Buried pipelines are critical infrastructure elements through which vital societal resources (*e.g.*, water, energy) are delivered. In seismic regions, buried pipelines are vulnerable to both wave propagation and permanent ground deformation (PGD) during earthquakes. In particular, failure to rapidly detect failures in a water distribution system can hamper emergency response efforts after an earthquake and could expose the public to contaminated water. The task of rapidly detecting damage in buried pipelines is challenging largely due to their subterranean location [1]. For example, buried pipelines are inaccessible for visual inspection. While non-contact sensing technologies such as infra-red thermography [2] and ground penetrating radar [3] allow inspectors to detect pipe leaks from above the ground surface, these technologies are difficult to master and are often expensive to operate.

While wave propagation and PGD can introduce damage in buried pipelines, PGD is widely regarded as the more destructive of the two [4]. A pipeline crossing an active fault is primarily subjected to bending and shear, but normal stress may result due to axial compression or tension of the pipeline. The precise behavior of the buried pipeline largely depends on its orientation relative to the fault plane. In the past three decades, a significant amount of research has been aimed at understanding the behavior of buried pipelines to PGD [5, 6]. Researchers have employed simplified models to describe the deformation modes of continuous and segmented buried pipelines [7-9]. In addition, detailed finite element analyses of pipelines subjected to PGD have also been reported in the literature [10]. Field evidence of pipe damage due to PGD have also led to empirical relationships between pipe type (*e.g.*, cast iron, concrete), characteristics of the PGD

*jerlynch@umich.edu; phone: (734) 615-5290; fax: (734) 764-4292; http://www-personal.umich.edu/~jerlynch/

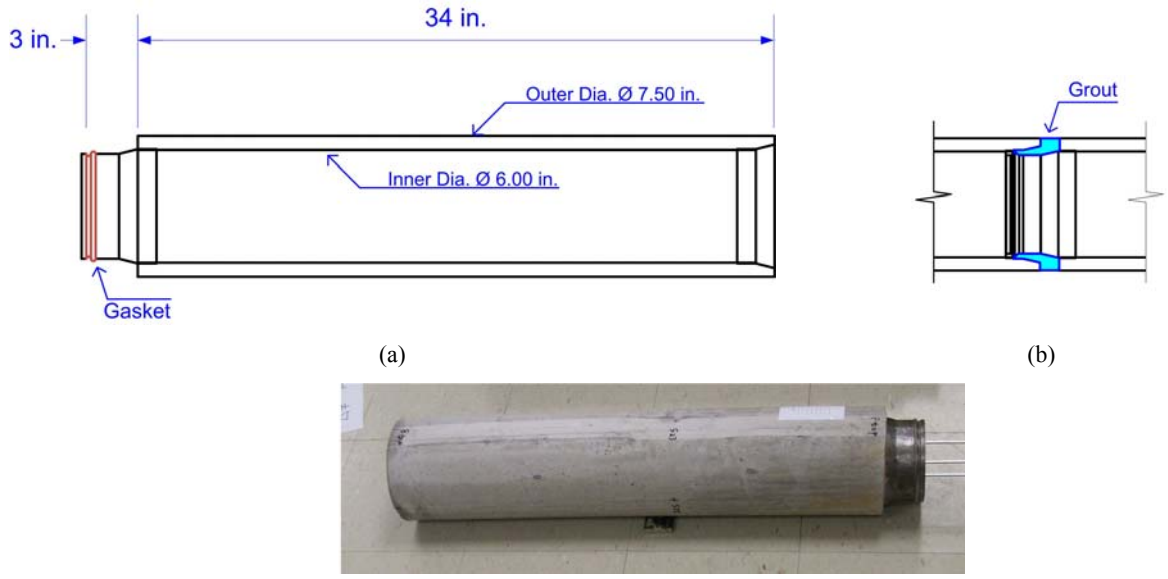

Fig. 1. Concrete pipe segment: (a) cross-section view of the pipe; (b) grouted connections; (c) picture of a typical pipe segment.

(*e.g.*, fault type, displacement), and damage severity (*e.g.*, number of breaks per unit length of pipeline) [11-13].

Undoubtedly, analytical modeling and field investigation have increased the field's understanding of continuous and segmented pipeline behavior under PGD. However, experimental testing of buried pipelines in controlled laboratory settings could further accelerate the technological development of durable pipelines that can safely withstand PGD. Large-scale testing of pipelines has been previously conducted with the majority of tests focusing on the behavior of metallic and high density polyethylene pipelines; comparatively less experimental work has been focused on segmented concrete pipelines. In this study, an experimental program focused on the behavior of segmented concrete pipelines is pursued. To explore the behavior of a segmented concrete pipeline during PGD, experimental testing is performed in the Lifeline Experimental and Testing Facility at Cornell University which is an experimental node of the Network for Earthquake Engineering Simulation (NEES). A dense array of sensors is installed along the length of the pipeline to measure its response to PGD introduced during fault displacement. First, the pipeline specimen is described followed by a detailed description of the experimental plan. Second, results from displacement-controlled loading of the pipeline are presented. The paper concludes with a summary of key experimental findings and a description of future research tasks.

2. EXPERIMENTAL SETUP

2.1 Pipeline Specimen

A one-fifth scale concrete pipe segment was designed and manufactured in compliance with the AWWA C2003 standards [14] for reinforced concrete pressure pipes. The pipe, as shown in Fig. 1, was designed with an inner diameter of 15.2 cm (6 in) and an outer diameter of 19.2 cm (7.5 in). The inner diameter of the pipe was lined with a thin steel sheet with the ends of the steel lining shaped to form a bell-spigot joint. Light steel hoop reinforcement was also spot welded to the outer surface of the steel lining before casting; a total of 21 #3 reinforcement bars were applied to the lining. Concrete was then cast on the outer surface of the steel lining to create a 2 cm (0.8 in) thick concrete wall spanning 86.4 cm (34 in). The concrete material consisted of 60% aggregate and self consolidating mortar with a water-to-cement ratio of 0.42. The self consolidating mortar also had 0.65% (by weight of cement) high-range water reducer. Testing of the concrete after 28 days revealed compressive strengths of about 60 MPa (8700 psi). The spigot joint of the steel lining protruded past the concrete wall an additional 7.6 cm (3 in). A rubber gasket was placed on the male end of

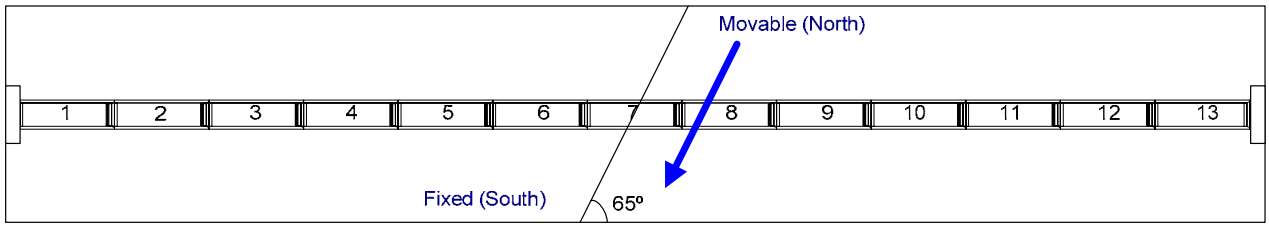

Fig. 2. Layout of the segmented concrete pipeline in the Lifeline Experimental and Testing Facility's test basin.

(a) (b) (c)

Fig. 3. (a) Empty test basin with a thin layer of compacted soil. (b) Assembled segmented concrete pipeline prior to backfilling. (c) Fully backfilled and compacted granular soil in the test basin prior to testing.

the steel lining to ensure the snug bell-spigot connection is snug during assembly of the pipeline. In total, thirteen pipes segments were constructed at the Materials Engineering Lab at Purdue University. The pipes were then shipped to the Lifeline Experimental and Testing Facility at Cornell University where they were assembled into a complete segmented pipeline. Assembly consisted of slipping the spigot (male) end of one pipe into the bell (female) end of another. Grout containing 30% fine aggregate, a 0.5 water-to-cement ratio, and 0.5% high-range water reducer, was mixed and poured into the annular spaces of each bell-spigot connection to fully seal the joint and to provide continuity of the concrete lining.

The segmented concrete pipeline was assembled in a large test basin at the Lifeline Experimental and Testing Facility (Fig. 2). The test basin was 1.9 m (6.2 ft) deep with an area of 11.7 m (38.4 ft) by 3.4 m (11.2 ft). The basin was designed to simulate a transverse fault oriented 65º relative to the longitudinal length of the basin. The north end of the test basin was attached to hydraulic actuators for controlled displacement while the south end of the basin was held fixed. The 13 pipe segments were installed along the longitudinal axis of the basin with the center pipe segment (designated as pipe segment #7 in Fig. 2) crossing the transverse fault. Given the angle of the fault plane, the pipe was placed in axial compression during simulated PGD; this required the pipe to be fixed at both ends of the basin without restricting end rotations. Granular soil was backfilled into the test basin to bury the pipeline roughly 115 cm (3.8 ft) beneath the soil surface. During backfilling, soil was added to the box in 20 cm thick layers with compaction applied between layers. During the backfilling stage, a nuclear density gauge was used to repeatedly measure the density and water content of the soil; a relatively constant density (1.7 Mg/m^3) and water content (5%) was observed throughout the soil column [15]. Fig. 3 provides views of the assembly process of the segmented concrete pipeline in the test basin.

2.2 Instrumentation Plan

To monitor the deformation and failure modes of the buried segmental concrete pipeline, a dense array of sensors were installed along the length of the pipeline. First, to measure the translational and rotational movement of individual pipe

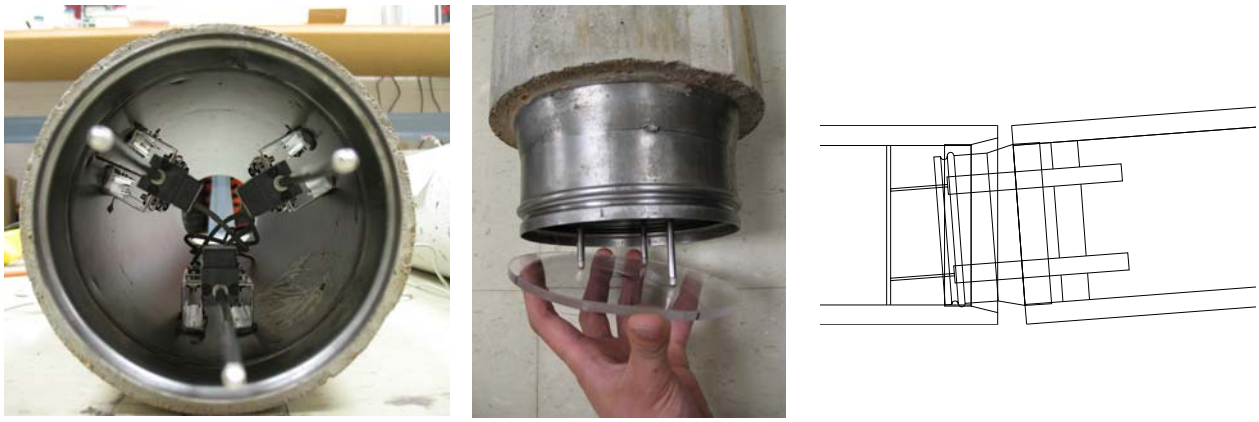

(a) (b) (c)

Fig. 4. (a) Three LVDTs mounted on C-channel blocks on the interior of the steel lining of the pipe segment. (b) The needles of the LVDTs cantilever past the lining and bear on a Lucite plate mounted in the adjacent segment. (c) The range of rotation measurements is limited by the point when one of the needles comes to the edge of the Lucite plate.

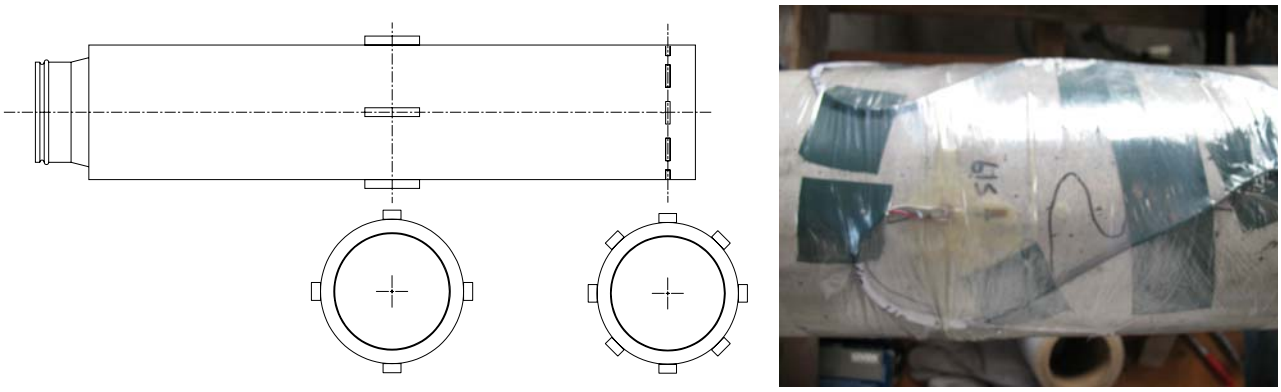

(a) (b)

Fig. 5. (a) Installation of strain gauges on the multiple pipe segments. Axial strain measured on 4 strain gauges mounted at the center of pipe segments #3 through #10. 8 additional strain gauges installed at the bell end of pipe segment #6 to measure hoop strain. (b) Strain gauge mounted to the surface of the concrete and wrapped in cellophane to protect it during testing.

segments, three linear variable differential transducers (LVDT) (Novotechnik TR100 LVDT) were installed at the pipe connections starting at the joint between segments #3 and #4 and ending at the joint between segments #10 and #11 (making a total of 8 joint segment connections instrumented). As shown in Fig. 4a, one LVDT was epoxy bonded to the bottom of the internal steel lining of each pipe segment's spigot end; two other LVDTs were installed 120º away from the bottom-most LVDT. The spring-loaded LVDTs were cantilevered past the end of each pipe segment to ensure that their needles could bear on a Lucite plate epoxy mounted at the end of the adjacent pipe segment (Fig. 4b). Averaging the three LVDTs displacement measurements provides a measure of the axial movement at the joint. The difference in measured displacement by the two LVDTs at the top of the pipe divided by the separation distance between their needles provides a measure of joint rotation. To provide ample room for rotation, the LVDTs were mounted on C-channel blocks roughly 3 cm (1.2 inch) tall. With a separation of 6.35 cm (2.5 in) between the top two LVDT needles, the maximum rotation angle that can be measured before the needles come to the edge of the Lucite plate is roughly 15º, as seen in Fig. 2c.

In addition to measuring joint deformation, axial and flexural strain were measured using strain gauges (Vishay L2A-06-250LW 350Ω metal foil gages) mounted longitudinally along the length of the pipeline (Fig. 5a). Specifically, 4 metal

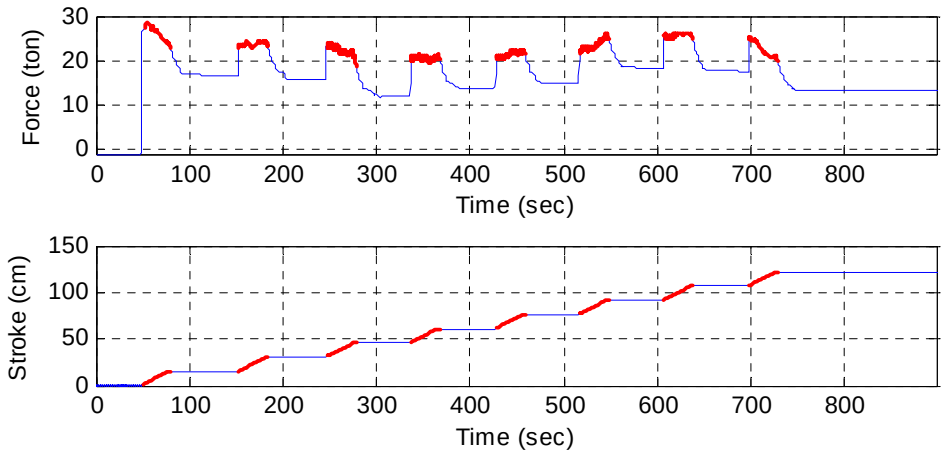

Fig. 6. Displacement-controlled actuation of the test basin: (top) total applied actuator force and (bottom) displacement time histories.

foil strain gauges were epoxy bonded to the concrete surface at the center of pipe segments #3 through #10. For each segment, two strain gauges were mounted to the top and bottom surface to measure axial strain while an additional two strain gauges were mounted on the two sides to measure flexural strain. After mounting, the strain gauges were protected from soil friction by wrapping the center of each concrete pipe segment in a single layer of cellophane (Fig. 5b). An additional 8 strain gauges were mounted circumferentially on the concrete surface of pipe segment #6 roughly 3.8 cm (1.5 in) from its bell (female) end. These eight gauges were installed to measure hoop strain at the pipeline connection closest (between segments #6 and #7) to the fault plane. At each of the two ends of the pipeline, 4 load cells were installed to measure the forces imparted to the test basin during compression deformation of the pipeline. Finally, the force and displacement output from the hydraulic actuators were also read during PGD testing.

The 24 LVDTs were interfaced to wireless sensor nodes (*Narada*) under development for structural health monitoring at the University of Michigan [16]. Furthermore, the 40 strain gauges, 4 load cells, and two hydraulic actuators were interfaced to the laboratory's National Instrument data acquisition system for data collection. One LVDT channel was also interfaced to the National Instrument data acquisition system to allow for synchronization between the LVDT channels collected by the wireless system and the other measurement channels collected by the wired system.

3. RESULTS

3.1 Testing Protocol

Ground faulting was simulated by displacement of the northern end of the test basin. Two hydraulic actuators operated under displacement-control were commanded to displace the northern end of the basin. The basin was displaced in increments of 15.25 cm (6 in) under a constant displacement rate of 0.5 cm/s (Fig. 6). After each displacement, the basin was held fixed for 60 second to allow for stress relaxation of the soil-pipe system. The box was displaced 8 times resulting in a maximum displacement of 1.22 m (48 in). Considering the slow movement of the northern portion of the test basin, a modest sample rate of 10 Hz was utilized during data acquisition. After the completion of the PGD test, the backfill soil was carefully removed and visual forensic analysis of the pipeline was conducted.

3.2 Visual Inspection after Permanent Ground Displacement

After the removal of the loose granular soil at the end of the test (Fig. 7a), the pipeline was visually inspected. Considerable damage was immediately witnessed in the vicinity of the fault plane. Specifically, the pipeline connection between segments #6 and #7 and segments #7 and #8 were evidently subjected to severe bending moment and axial force. Failure at these joints led to complete separation of pipe segment #7 from segments #6 and #8 (Fig. 7b). In addition, the severe shear force distorted the center pipe segment into an oval shape with the concrete wall completely spalled from the steel sleeve (Fig. 7c). The joint between pipe segments #8 and #9 also experienced some telescopic failure with the spigot telescoping into the bell of the adjacent pipe (Fig. 7d). The telescopic failure was attributed to

Fig. 7. (a) Excavated pipeline after PGD. Central pipe segement #7 was completely removed from segments #6 and 8. (b) The joint between segements #7 and 8 with LVDT needle evident. (c) Oval distortion of segment #7 due to extreme shear forces during PGD. (d) Telescopic failure at the connection between segement #8 and #9.

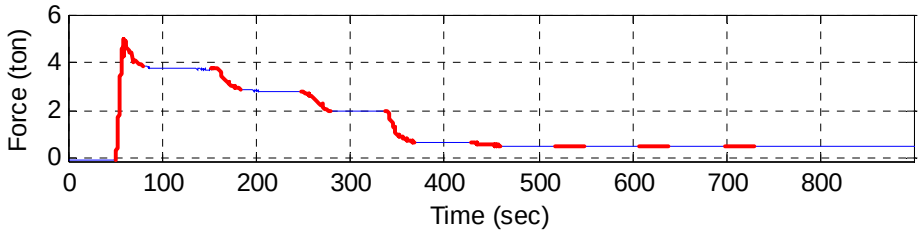

Fig. 8. Axial force measured at the southern end of the test basin. A noticeable reduction in the axial force is witnessed 8 sec into the first actuation step (corresponding to a displacement of 5.2 cm on the fault plane).

high compressive forces that developed during PGD. The portions of the pipeline away from the fault plane appeared undamaged which further supports the assumption that damage in the pipeline was largely localized to the center pipe segment crossing the fault plane.

3.3 Analysis of the Pipeline Measured Response

The concrete segmented pipeline was subjected to flexural bending and axial compression during the early stages of actuation. The axial compressive force (Fig. 8) measured at the southern end of the pipeline grew rapidly until a sudden drop was witnessed at about 8 seconds into the first displacement step. This distinct change in axial force measured at the end of the pipeline corresponded to a PGD of 5.2 cm. The sudden drop in axial force suggested severe structural damage along the pipeline; the most likely cause was the damage withstood by pipe segment #7 including cover spalling and destruction in the vicinity of the segment's joints. Investigation of the actuation force (Fig. 6) corroborates this

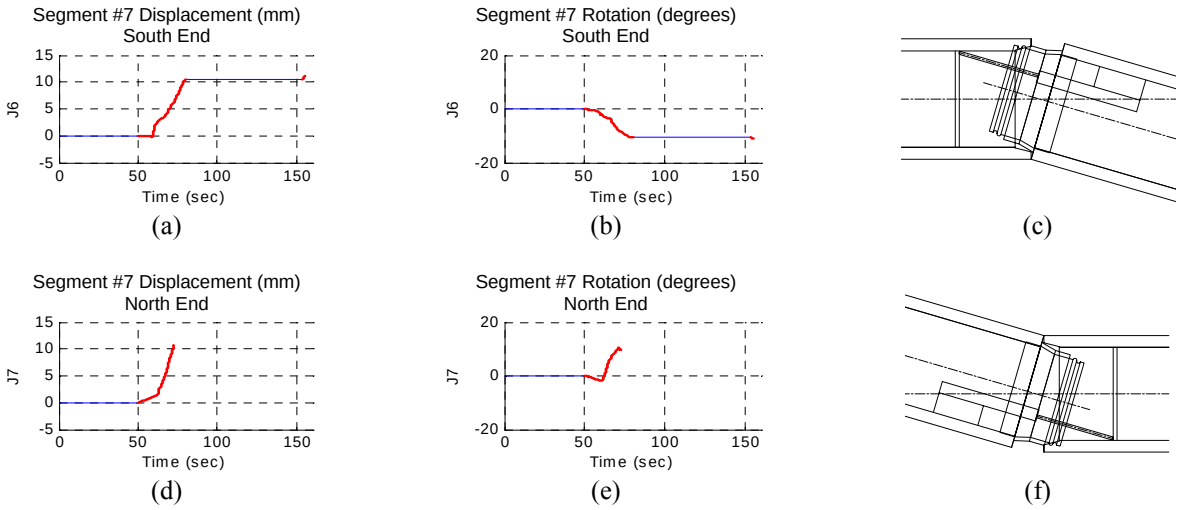

Fig. 9. Response of pipe segment #7: (a) south-end displacement; (b) south-end rotation; (c) LVDT at the limit of its measurement range at the southern-end; (d) north-end displacement; (e) north-end rotation; (f) LVDT at the limit of its measurement range at the northern-end.

interpretation of the pipeline behavior. For example, the actuation force was initially large as the pipeline underwent flexural bending. The actuation force peaked at 29 tons and decreased thereafter due to the softening of the joints at the ends of pipe segment #7. During subsequent actuation steps, the axial force (Fig. 8) continued to reduce suggesting the release of axial stress in the pipeline. After the fourth actuation step, the axial force ceased to decrease, suggesting that the center pipe segment was fully detached from pipeline.

Investigation of the LVDTs at the ends of the pipe segments further revealed the behavior of the pipeline during the first actuation step. The majority of instrumented connections showed negligible displacement and rotation during loading. Only three connections revealed noteworthy deformation during fault displacement. For example, the displacement and rotation of the southern and northern joints of pipe segment #7 during the first actuation step are presented in Fig. 9. Only LVDT measurements from the first actuation step were reliable due to the LVDT needles coming to the edge of the Lucite plates toward the end of the actuation step (Fig. 9c and 9f). The final rotation at the south- and north-ends of pipe segment #7 was 11.6º and 10.5º, respectively, while the axial compressive displacement was 10.8 and 10.2 mm, respectively. The joint between pipe segment #8 and 9 also experienced 2.5 mm of compressive displacement and a modest rotation of 3º; this was the joint with telescopic damage.

The strain gauges in the center of pipe segments in the vicinity of the fault plane provided additional insight to the behavior of the pipeline during the first actuation step. As shown in Fig. 10, the axial strain (calculated from an average of the top and bottom strain gauges) and bending strain (calculated as the difference between the two strain gauges on the side of the segments) of pipe segments #6 and #8 are plotted. The strain time histories revealed that both pipe segments were subjected to axial compression and flexural bending. However, there was a sudden spike and drop roughly 6 seconds into the first actuation step suggesting structural damage somewhere along the pipeline. A similar trend was also found in the circumferential strain measured at the bell-end of pipe segment #6 (Fig. 10c). The circumferential strain grew steadily until about 8 seconds into the first actuation step when many of the gages suddenly jumped to large levels of strain (1800 με) and then settled down to a residual level of 1200 με. This behavior is consistent severe cracking near the circumferential strain gauges at the connection between pipe segments #6 and #7.

4. CONCLUSIONS

This study explored the behavior of a buried concrete segmented pipeline exposed to permanent ground displacement. In total, 13 one-fifth scale concrete pipe segments were assembled into a continuous pipeline within a large test basin at Cornell University's Lifeline Experimental and Testing Facilities. The pipeline was covered with a 115 cm thick layer of loose granular soil consolidated to a density of 1.7 Mg/m^3. Two hydraulic actuators were used to displace half of the

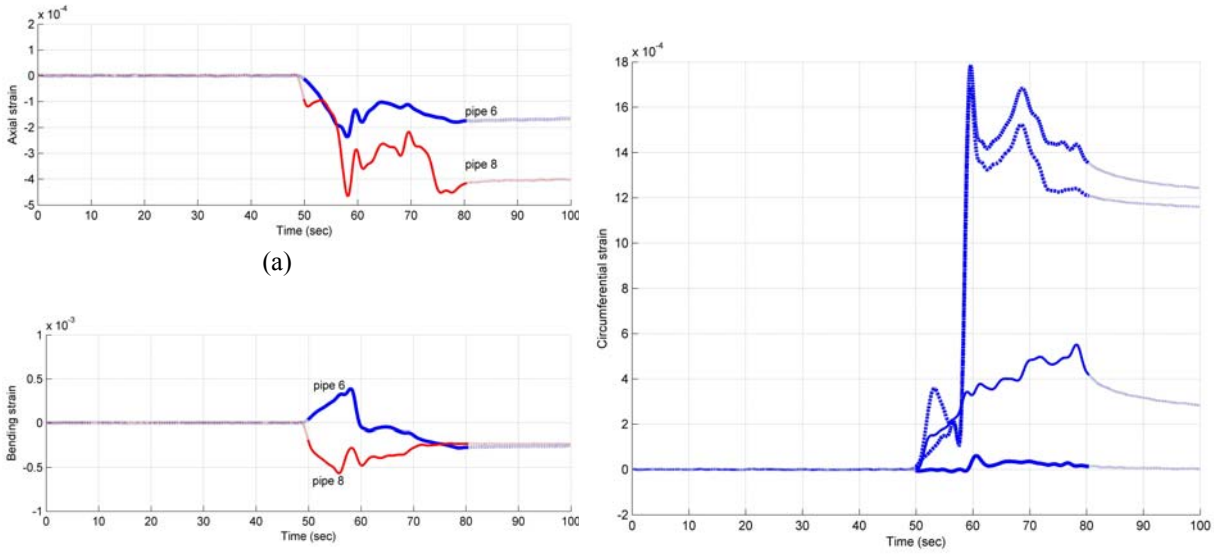

Fig. 10. Pipeline strain response during the first actuation step: (a) axial strain of pipe segments #6 and #8; (b) bending strain of pipe segments #6 and 8; (c) four channels of circumferential strain measured at the bell-end of pipe segment #6.

test basin in 8 increments of 15.25 cm each. Joint rotation and axial displacement was measured at each joint while load cells were used to measure axial loads at the two ends of the pipeline. In addition, strain gauges were installed at the center of pipes to measure axial and bending strains.

Based on the analysis of the sensor data, it was evident that the pipeline deformation was concentrated to the two ends of the pipe segment crossing the fault plane (segment #7). At 8 seconds into the first actuation step, cracking at the joint between segments #6 and 7 was observed from the circumferential strain measurements. At the same time, a dramatic reduction in the axial compression was witnessed at the south-end of the pipeline. Using the displacement and rotation measurements made at the center pipe segment, the deflected shape of the pipe is drawn in Fig 11. The deflected shape pipeline segments #6, #7 and #8 are plotted as measured (dark line); for comparison, the deflected shape of the pipeline assuming pipe segment #7 was connected with pin connections at its two ends is superimposed (gray line). As can be seen in Figure 11, the measured deflected shape is nearly identical to the situation of a pin-ended segment #7. This supports the conclusion that severe damage at the ends of segment #7 is the primary cause of failure of the pipeline reducing pipe segment #7 to a pin-ended segment. The pipe was severely damaged by a fault displacement of 5.2 cm which was well below what was anticipated for the concrete segmented pipeline. The design of the bell-spigot connection was the likely culprit for premature failure of the pipeline.

A primary objective of this study was to observe the modes of failure of concrete segmented pipelines under permanent ground displacement. The study was successful in observing severe damage in the bell-spigot joints of the pipe segement crossing the fault. Observations made during these tests will direct future research. For example, plans are already underway for the testing of a commercial concrete segmented in 2009. It is anticipated that a commercial pipeline will have more steel reinforcement offering significantly more confinement of the concrete in the bell-spigot connection. It is hoped that more flexural behavior in the pipeline will be observed during these tests.

ACKNOWLEDGMENTS

This research was sponsored by the National Science Foundation under the NEES Program (Grant CMMI-0724022). We would like to thank the Cornell staff for helping with the experiment. In particular, we acknowledge the help of Mr. Tim

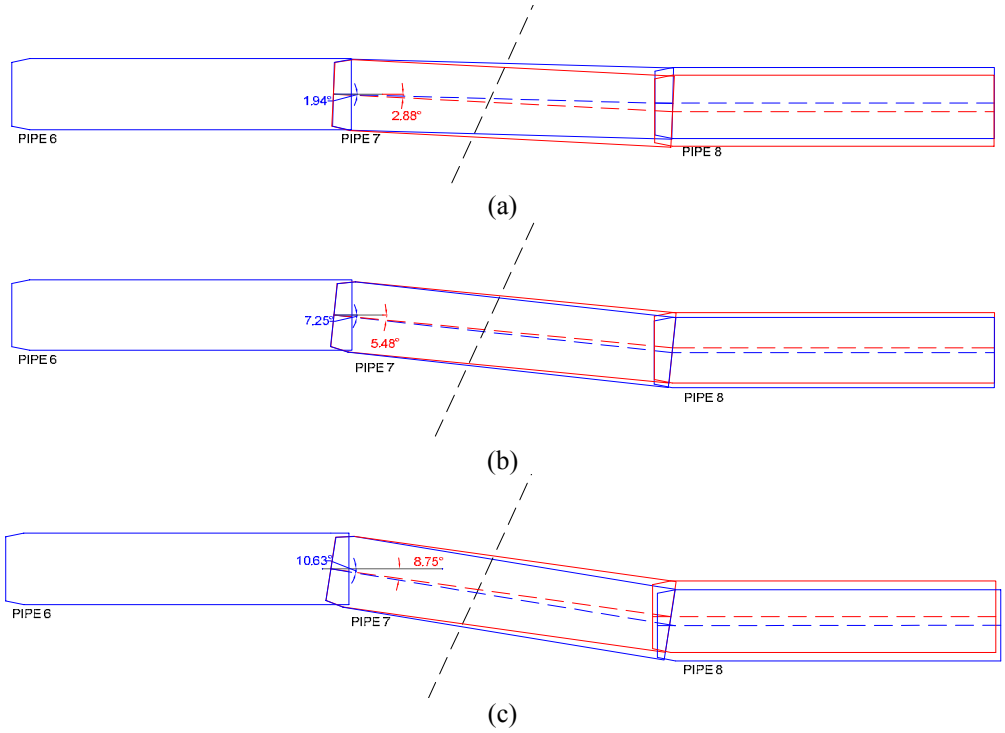

Fig. 11. Tracking the movement of pipe segments #6, #7 and #8 during the first actuation step: (a) 10 seconds, (b) 20 seconds, and (c) at the instant of reaching the sensing limit of the LVDTs.

Bond, manager of operations of the Harry E. Bovay Jr. Civil Infrastructure Laboratory Complex at Cornell University, and Mr. Joe Chipalowski, the manager of Cornell's NEES Equipment Site. We also thank Professor Tom O'Rourke for his participation. Additional thanks go to Ms. Qinge Ma, and Mr. John Davis their support, and to Cornell graduate students Nathan Olson and Jeremiah Jezerski for sharing their expertise during preparation of the pipeline test.

REFERENCES

[1] O'Rourke, T. D., "Soil-structure interaction under extreme loading conditions", 13th Spencer J. Buchanan Lecture, Texas A&M University, College Station, TX (2005).

[2] Inagaki, T. and Okamoto, Y., "Diagnosis of the leakage point on a structure surface using infrared thermography in near ambient conditions", NDT&E International, 30 (3), 135-142 (1997).

[3] Hayakawa, H. and Kawanaka, A., "Radar imaging of underground pipes by automated estimation of velocity distribution versus depth", Journal of Applied Geophysics, 40 (1-3), 47-48 (1998).

[4] Eguchi, R. T., "Seismic vulnerability models for underground pipes", In: [Earthquake behavior and safety of oil and gas storage facilities, buried pipelines and equipment], ASME, New York, NY, 368-373 (1983).

[5] Isoyama, R. and Katayama, T., [Reliability evaluation of water supply systems during earthquakes], Institute of Industrial Science, University of Tokyo, Tokyo, Japan (1982).

[6] Markov, I., Grigoriu, M. and O'Rourke, T. D., [An evaluation of seismic serviceability of water supply networks with application to san francisco auxiliary water supply system], National Center for Earthquake Engineering Research, Buffalo, NY (1994).

[7] Newmark, N. M. and Hall, W. J., "Pipeline design to resist large fault displacement", Proceedings of the 1975 US National Conference on Earthquake Engineering, 416-425, Ann Arbor, MI (1975).

[8] Kennedy, R. P., Chow, A. W. and Williamson, R. A., "Fault movement effects on buried oil pipeline", Journal of the Transportation Engineering Division, 103 (TE5), 617-633 (1977).

[9] O'Rourke, T. D., Grigoriu, M. D. and Khater, M. M., "A state of the art review: Seismic response of buried pipelines", In: [Decade of progress in pressure vessel technology], ASCE, New York, NY, (1985).

[10] Yoshisaki, K., O'Rourke, T. D. and Hamada, M., "Large deformation behavior of buried pipelines with low-angle elbows subjected to permanent ground deformation", Journal of Structural Mechanics and Earthquake Engineering, 50 (4), 215-228 (2001).

[11] Porter, K. A., Scawthorn, C., Honegger, D. G., O'Rourke, T. D. and Blackburn, F., "Performance of water supply pipelines in liquefied soil", Proceedings of the 4th US-Japan Workshop on Earthquake Disaster Prevention for Lifeline Systems, 3-17, Los Angeles, CA (1991).

[12] Eidinger, J. M., Maison, B., Lee, D. and Lau, B., "East bay municipal utility district water distribution damage in 1989 Loma Prieta earthquake", Proceedings of the 4th US Conference on Lifeline Earthquake Engineering, 240-247, San Francisco, California (1995).

[13] O'Rourke, T. D., Toprak, S. and Sano, Y., "Factors affecting water supply damage caused by the Northridge Earthquake", Proceedings of the 6th US National Conference on Earthquake Engineering, Seattle, WA (1998).

[14] AWWA, [C300 standard for reinforced concrete pressure pipe, steel cylinder type, for water and other liquids], American Water Works Association Denver, CO (2004).

[15] Bradshaw, A. S., DaSilva, G., McCue, M. T., Kim, J., Nadukuru, S. S., Lynch, J. P., Michalowski, R., Pour-Ghaz, M., Weiss, J. and Green, R. A., "Damage detection and health monitoring of buried concrete pipelines", Proceedings of the International Symposium on the Prediction and Simulation Methods for Geohazard Mitigation, Kyoto, Japan (2009).

[16] Swartz, R. A., Jung, D., Lynch, J. P., Wang, Y., Shi, D. and Flynn, M. P., "Design of a wireless sensor for scalable distributed in-network computation in a structural health monitoring system", 5th International Workshop on Structural Health Monitoring, 1570-1577, Stanford, CA (2005).